Thermal Boundary Layer Equation for Turbulent Rayleigh–Bénard Convection

Olga Shishkina,* Susanne Horn,† and Sebastian Wagner
Max Planck Institute for Dynamics and Self-Organization, Am Fassberg 17, D-37077 Göttingen, Germany

Emily S. C. Ching‡
Department of Physics, The Chinese University of Hong Kong, Shatin, Hong Kong

(Dated: January 16, 2015)

We report a new thermal boundary layer equation for turbulent Rayleigh–Bénard convection for Prandtl number $\mathcal{P}r > 1$ that takes into account the effect of turbulent fluctuations. These fluctuations are neglected in existing equations, which are based on steady-state and laminar assumptions. Using this new equation, we derive analytically the mean temperature profiles in two limits: (a) $\mathcal{P}r \gtrsim 1$ and (b) $\mathcal{P}r \gg 1$. These two theoretical predictions are in excellent agreement with the results of our direct numerical simulations for $\mathcal{P}r = 4.38$ (water) and $\mathcal{P}r = 2547.9$ (glycerol) respectively.

PACS numbers: 44.20.+b, 44.25.+f, 47.27.ek, 47.27.te

arXiv:1411.5826v2 [physics.flu-dyn] 15 Jan 2015

Turbulent Rayleigh–Bénard convection (RBC) [1–5], consisting of a fluid confined between two horizontal plates, heated from below and cooled from above, is a system of great research interest. It is a paradigm system for studying turbulent thermal convection, which is ubiquitous in nature, occurring in the atmosphere and the mantle of the Earth as well as in stars like our Sun. Convective heat transfer is also an important problem in engineering and technological applications. The state of fluid motion in RBC is determined by the Rayleigh number $\mathcal{R}a = \alpha g \Delta H^3/(\kappa\nu)$ and Prandtl number $\mathcal{P}r = \nu/\kappa$. Here α denotes the isobaric thermal expansion coefficient, ν the kinematic viscosity and κ the thermal diffusivity of the fluid, g the acceleration due to gravity, Δ the temperature difference between the bottom and top plates, and H the distance between the plates.

In turbulent RBC, there are viscous boundary layers (BLs) near all rigid walls and two thermal BLs, one above the bottom plate and one below the top plate. We denote the thicknesses of the viscous and thermal BLs by l and λ respectively. Both viscous and thermal BLs play a critical role in the turbulent heat transfer of the system and in particular λ is inversely proportional to the heat transport. Grossmann and Lohse (GL) [6], [7] developed a scaling theory of how the Reynolds number $\mathcal{R}e$, determined by the mean large-scale circulation velocity U_0 above the viscous BL, and the dimensionless Nusselt number $\mathcal{N}u$, measuring the heat transport, depend on $\mathcal{R}a$ and $\mathcal{P}r$ for moderate $\mathcal{R}a$. The theory makes explicit use of the result $l/H \propto \mathcal{R}e^{-1/2}$ with the proportionality constant depending only on $\mathcal{P}r$. This result follows from the assumptions that the BLs are laminar and their mean profiles, averaged over time, are described by the Prandtl–Blasius–Pohlhausen (PBP) theory [8–10] for steady-state forced convection above an infinite weakly-heated plate. Although the GL theory gives perfect agreement with the heat transport measurements, the assumption that the BLs are described by PBP theory is not fulfilled. Systematic deviations of the mean velocity and temperature profiles from the PBP predictions have been reported both in experiments and in direct numerical simulations (DNS) [11–15]. These deviations remain even after a dynamical rescaling procedure [16] that takes into account of the time variations of λ is used, and increase with growing $\mathcal{R}a$ and decreasing $\mathcal{P}r$. An extension of the PBP approach to the Falkner–Skan–Pohlhausen one [17–19], which accounts for a non-parallel mean large-scale circulation velocity above the viscous BL [20] and a non-zero pressure gradient within the BLs, gives better approximations of l and λ [19] and is promising for studying mixed convection [21, 22] but does not lead to better predictions of the mean temperature profiles in RBC. For large $\mathcal{P}r$, the thermal BL is nested within the viscous one. Taking the velocity field to be a simple shear flow with constant shear rate, Shraiman and Siggia [23] obtained results for the mean temperature profile and the relation between the heat flux and shear rate. Their mean temperature profile coincides with the PBP prediction for $\mathcal{P}r \gg 1$. Ching [24] generalized their work to study shear flows with position-dependent shear rate, and obtained mean temperature profiles in terms of two constants that are functions of λ, the shear rate and their spatial derivatives. Good agreement of the derived profile with the actual ones can be obtained only when these two constants are treated as free fitting parameters with no solid theoretical support.

The observed deviations between the actual profiles and the existing predictions from laminar BL models are the effects of turbulent fluctuations. As $\mathcal{R}a$ increases, the present understanding is that the thermal BLs would eventually become turbulent such that a clear distinction between the BLs and the bulk of the flow ceases to exist. In this asymptotic state, known as the ultimate regime, logarithmic mean temperature profiles are predicted [25] based on the idea of eddy thermal diffusivity [10]. Recently, logarithmic mean temperature profiles in the turbulent bulk region have also been reported for moderate $\mathcal{R}a$ [26]. The separation of the region close to the plate

into a viscous sublayer and a fluctuating logarithmic layer [25, 26] gives a good description of the mean temperature profile in these two separate subregions but a universal function predicting correctly the mean temperature profile throughout the whole region, from the plate to the edge of the bulk region, remains lacking.

In this Letter, we report a new thermal BL equation for turbulent RBC that takes into account the effect of the turbulent fluctuations, which are neglected in the existing BL equations based on steady-state and laminar assumptions. Using this equation, we derive analytically the mean temperature profiles for $\mathcal{P}r \gtrsim 1$ and $\mathcal{P}r \gg 1$. We have performed DNS for $\mathcal{P}r = 4.38$ (water) and $\mathcal{P}r = 2547.9$ (glycerol) with $\mathcal{R}a$ between 10^7 and 10^{10} in a cylindrical domain of aspect ratio one, using well-tested finite-volume codes. The DNS for $\mathcal{R}a$ up to 10^9 were conducted using the RBC-version [27] of the code [28]. The simulations for higher $\mathcal{R}a$ were obtained using our new code *goldfish*, which features a versatile operator approach, a high modularity and fully parallel I/O and was validated against [27] for $\mathcal{R}a = 10^8$. The computational grids used resolve Kolmogorov and Batchelor scales in the whole domain [29]. Our theoretical predictions are in excellent agreement with our DNS results.

We consider the fluid flow along an infinite horizontal heated plate and assume that far away from the plate there exists a constant horizontal mean velocity, the wind, along a certain preferential direction. We set up the coordinate system such that the x-direction is along the wind and z-direction is vertical away from the plate. As the dependence of the mean flow on the other horizontal direction is weak when the plate is large, we consider a two-dimensional flow that depends on x and z only. Denote the velocity field by $u(x,z,t)\hat{x} + v(x,z,t)\hat{z}$ and the temperature field by $T(x,z,t)$, where $\hat{x}$ and $\hat{z}$ are the unit vectors in the corresponding directions and t is the time. Close to that plate the equation of motion of temperature is governed by

$$\partial_t T + u\partial_x T + v\partial_z T = \kappa\partial_z^2 T, \tag{1}$$

where we have used the BL approximation of $|\partial_x^2 T| \ll |\partial_z^2 T|$. Applying Reynolds decomposition, we can write the velocity and temperature fields as the sums of their long time averages, denoted by $U(x,z)$, $V(x,z)$ and $\Theta(x,z)$, and their fluctuations defined by

$$u(x,z,t) = U(x,z) + u'(x,z,t), \tag{2}$$
$$v(x,z,t) = V(x,z) + v'(x,z,t), \tag{3}$$
$$T(x,z,t) = \Theta(x,z) + \theta'(x,z,t). \tag{4}$$

Here $U(x,z) \to U_0$ as $z \to \infty$. Taking a long time average, denoted by $\langle\cdot\rangle_t$, of (1), we obtain

$$U\partial_x\Theta + V\partial_z\Theta + \partial_x\langle u'\theta'\rangle_t + \partial_z\langle v'\theta'\rangle_t = \kappa\partial_z^2\Theta, \tag{5}$$

Assuming that $|\partial_x\langle u'\theta'\rangle_t| \ll |\partial_z\langle v'\theta'\rangle_t|$ and using the eddy thermal diffusivity $\kappa_t = \kappa_t(x,z)$, defined as

$$\langle v'\theta'\rangle_t \equiv -\kappa_t\partial_z\Theta, \tag{6}$$

one obtains the following BL equation

$$U\partial_x\Theta + (V - \partial_z\kappa_t)\partial_z\Theta = (\kappa + \kappa_t)\partial_z^2\Theta. \tag{7}$$

We seek a similarity solution of the BL equation (7) with respect to the similarity variable ξ, defined by

$$\xi = z/\lambda(x), \tag{8}$$

where $\lambda(x)$ is the local thickness of the thermal BL. Let the stream function $\Psi(x,z)$ for the mean velocity be

$$\Psi(x,z) = U_0\lambda(x)\psi(\xi), \tag{9}$$

such that $U = \partial_z\Psi$ and $V = -\partial_x\Psi$, and $\Theta(x,z)$ be

$$\Theta = T_{bot} - (\Delta/2)\theta(\xi). \tag{10}$$

Here T_{bot} is the temperature of the bottom plate. The boundary conditions for ψ and θ are

$$\psi(0) = 0, \qquad \psi_\xi(0) = 0, \qquad \psi_\xi(\infty) = 1, \tag{11}$$
$$\theta(0) = 0, \qquad \theta_\xi(0) = 1, \qquad \theta(\infty) = 1. \tag{12}$$

Here the subscript ξ denotes the derivative with respect to ξ. Using (8)–(10) in (7) one obtains the following dimensionless BL equation

$$(1 + \kappa_t/\kappa)\theta_{\xi\xi} + (A + B\psi)\theta_\xi = 0, \tag{13}$$
$$A = (\kappa_t)_\xi/\kappa, \quad B = U_0\lambda\lambda_x/\kappa. \tag{14}$$

and the subscript x denotes the derivative with respect to x. For the similarity solution to exist, B must be constant, independent of x, therefore $\lambda(x) \propto \sqrt{x}$. In the BL approximation, $l \propto \lambda$ and thus $l \propto \sqrt{x}$ as in PBP theory and is therefore consistent with the assumption used in GL scaling theory [6] for moderate $\mathcal{R}a$. We write

$$\lambda(x) = f\sqrt{\nu x/U_0} \tag{15}$$

and thus $B = \mathcal{P}r f^2/2$, where $f = f(\mathcal{P}r)$ is some function of $\mathcal{P}r$ that is fixed by the requirement $\theta_\xi(0) = 1$.

In the case where fluctuations are ignored, $\langle v'\theta'\rangle_t = 0$, $\kappa_t = 0$, then (13) reduces to the PBP equation. It was derived in Shishkina *et al.* [18] that the PBP equation can be written as

$$\theta_{\xi\xi} + \omega\Gamma^\omega\left(1 + \omega^{-1}\right)\xi^{\omega-1}\theta_\xi = 0 \tag{16}$$

with $\omega = 2$ for $\mathcal{P}r \ll 1$ and $\omega = 3$ for $\mathcal{P}r \gg 1$ and thus all PBP temperature profiles for any $\mathcal{P}r$ are bounded by

$$\theta(\xi) = \int_0^\xi \exp\left[-\Gamma^\omega\left(1 + \omega^{-1}\right)\chi^\omega\right]\,\mathrm{d}\chi, \tag{17}$$

with $2 \le \omega \le 3$ where Γ is the gamma function. To take into account the fluctuations, we need to know $\kappa_t(\xi)$. A

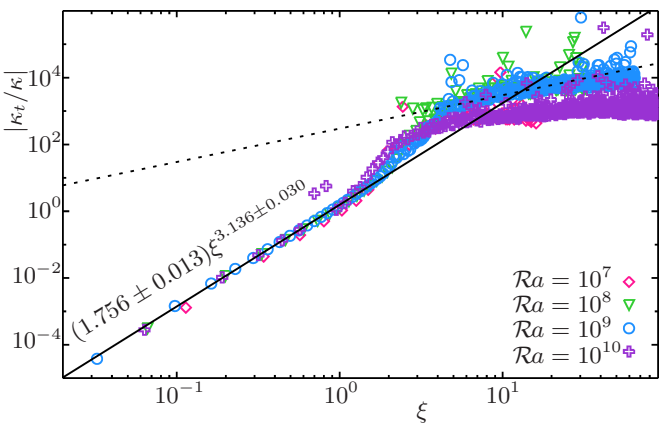

FIG. 1. Normalized eddy thermal diffusivity $|\kappa_t/\kappa|$, calculated for $\kappa_t = (V\Theta - \langle vT\rangle_t)/\partial_z\Theta$, and then averaged over horizontal cross-sections, obtained in the DNS for $\mathcal{P}r = 4.38$ and $\mathcal{R}a = 10^7$ (diamonds), 10^8 (triangles), 10^9 (circles) and 10^{10} (pluses) together with a fit for $\mathcal{R}a = 10^9$ (solid line). It can be seen that close to the plate, $\kappa_t/\kappa \propto \xi^3$ holds. Dashed line shows the slope $\propto \xi$ that causes the logarithmical temperature profiles in the core part of the domain for sufficiently large $\mathcal{R}a$.

common approach for fully turbulent BLs is $\kappa_t \propto \xi$ [10] consequently leading to logarithmic temperature profiles. For moderate $\mathcal{R}a$, such log-profiles are also found but only in the turbulent bulk, which is at a relatively large distance from the plate. In the vicinity of the plate κ_t behaves rather as $\kappa_t \propto \xi^3$ (see Fig. 1). Indeed, from the continuity equation for the fluctuating velocities, $\partial_x u' + \partial_z v' = 0$, and that θ', v' and $\partial_x u'$ vanishing at the plate, we obtain for $z = 0$:

$$\langle v'\theta'\rangle_t = \partial_z\langle v'\theta'\rangle_t = \partial_z^2\langle v'\theta'\rangle_t = 0. \tag{18}$$

Using the relation (6) and (8), (18) implies

$$\kappa_t(0) = (\kappa_t)_\xi(0) = (\kappa_t)_{\xi\xi}(0) = 0. \tag{19}$$

Therefore the following approximation

$$\kappa_t/\kappa \approx a^3\xi^3 \tag{20}$$

holds for small ξ with some dimensionless constant a. Substituting (14) and (20) into (13), one obtains the following BL equation for the temperature:

$$(1 + a^3\xi^3)\theta_{\xi\xi} + (3a^3\xi^2 + B\psi)\theta_\xi = 0. \tag{21}$$

For large $\mathcal{P}r$, the thermal BL is nested within the viscous BL such that $\lambda < l$ and we can approximate $U \propto z$ within the thermal BL. Together with (8)–(12), one obtains

$$\psi \approx b\xi^2, \quad b = 0.5\psi_{\xi\xi}(0). \tag{22}$$

(22) and (21) lead to the following new thermal BL equation for large $\mathcal{P}r > 1$:

$$(1 + a^3\xi^3)\theta_{\xi\xi} + (3a^3 + bB)\xi^2\theta_\xi = 0. \tag{23}$$

The solution of (23) is

$$\theta(\xi) = \int_0^\xi (1 + a^3\eta^3)^{-c} d\eta \tag{24}$$

with $c = \frac{bB}{3a^3} + 1$. Note that the constants a and c are related by the requirement $\theta(\infty) = 1$, which gives

$$a = \frac{\Gamma(1/3)\,\Gamma(c - 1/3)}{3\Gamma(c)}. \tag{25}$$

The order of magnitude of a can be estimated as follows. Averaging (5) in the x-direction, denoted by $\langle\cdot\rangle_x$, and integrating it in the vertical direction from 0 to z, and using (6) and the definition of the Nusselt number

$$\mathcal{N}u \equiv (\langle vT\rangle_{tx} - \kappa\partial_z\langle T\rangle_{tx})/(\kappa\Delta/H), \tag{26}$$

one obtains

$$\langle V\Theta\rangle_x = \langle(\kappa + \kappa_t)\partial_z\Theta\rangle_x + \mathcal{N}u\,\kappa\Delta/H. \tag{27}$$

Close to the plate, the order of magnitude of the left-hand side of (27) is much smaller than $\mathcal{N}u\,\kappa\Delta/H$, hence, in this region the following approximation holds:

$$\langle(\kappa + \kappa_t)\partial_z\Theta + \kappa\Delta/(2\lambda)\rangle_x \approx 0, \tag{28}$$

where we have used the definition

$$\lambda(x) \equiv -\partial_z\Theta\big|_{z=0}/(\Delta/2) \tag{29}$$

to write $\mathcal{N}u = \langle H/(2\lambda)\rangle_x$. Approximate that (28) holds locally, without the averaging in x, in the region far away from the two vertical walls, we get

$$\kappa/(\kappa + \kappa_t) \sim -(2\lambda/\Delta)\partial_z\Theta = \theta_\xi \tag{30}$$

(see Fig. 2). Our DNS show that at the edge ($\xi = 1$) of the thermal BL, $0.36 < \theta_\xi < 0.65$ holds for all $\mathcal{P}r$ studied. From (20) and (30) for $\xi = 1$ one obtains that $0.52 < a^3 < 1.76$, with $a \sim 1.2$ for $\mathcal{P}r \gtrsim 1$ and $a \sim 0.8$ for $\mathcal{P}r \gg 1$. Thus we have $c \sim 1$ for $\mathcal{P}r \sim 1$ and $c \sim 2$ for $\mathcal{P}r \gg 1$.

The analytical solution (24) of the BL equation (23) that satisfies (12) for $c = 1$ reads

$$\theta = \frac{\sqrt{3}}{4\pi}\log\frac{(1+a\xi)^3}{1+(a\xi)^3} + \frac{3}{2\pi}\arctan\left(\frac{4\pi}{9}\xi - \frac{1}{\sqrt{3}}\right) + \frac{1}{4}, \quad a = 2\pi/(3\sqrt{3}) \approx 1.2, \tag{31}$$

while that for $c = 2$ is

$$\theta = \frac{\sqrt{3}}{4\pi}\log\frac{(1+a\xi)^3}{1+(a\xi)^3} + \frac{3}{2\pi}\arctan\left(\frac{8\pi}{27}\xi - \frac{1}{\sqrt{3}}\right) + \frac{\xi}{3(1+(a\xi)^3)} + \frac{1}{4}, \quad a = 4\pi/(9\sqrt{3}) \approx 0.8. \tag{32}$$

Thus, all temperature profiles for $\mathcal{P}r > 1$ lie between (31) ($\mathcal{P}r \gtrsim 1$) and (32) ($\mathcal{P}r \gg 1$).

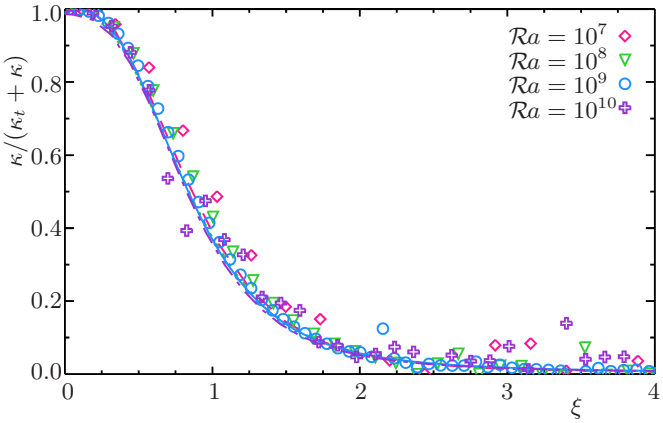

FIG. 2. $\kappa/(\kappa+\kappa_t)$ (symbols) [κ_t is calculated as in Fig. 1], and θ_ξ (lines), averaged in time and over horizontal cross-sections, as functions of the dimensionless vertical coordinate ξ [see definition in (8)] obtained in the DNS for $\mathcal{P}r = 4.38$ and $\mathcal{R}a = 10^7$ (diamonds, dashed line), 10^8 (triangles, dotted line), 10^9 (circles, solid line), 10^{10} (pluses, dot-dashed line).

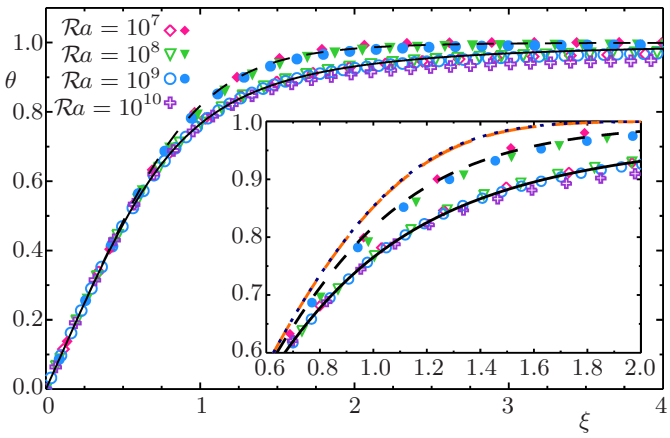

FIG. 3. Temperature profiles, averaged in time and over horizontal cross-sections, obtained in the DNS for $\mathcal{P}r = 4.38$ (open symbols) and $\mathcal{P}r = 2547.9$ (filled symbols) and $\mathcal{R}a = 10^7$ (diamonds), 10^8 (triangles), 10^9 (circles) and 10^{10} (pluses). Excellent agreement with the predictions for $\mathcal{P}r \gtrsim 1$ (31) (solid line) and $\mathcal{P}r \gg 1$ (32) (dashed line) is demonstrated. An expanded view with the PBP prediction (17) for $\mathcal{P}r = 2547.9$ (dotted line) and $\mathcal{P}r = 4.38$ (long-dashed orange line, which almost coincides with the dotted line) for comparison is shown in the inset.

Next we compare our predictions (31), (32) with the DNS results. At each of the two $\mathcal{P}r$ (4.38 and 2547.9) studied, the mean temperature profiles almost collapse for the different $\mathcal{R}a$ (10^7 to 10^9). Generally the profiles depend very weakly on $\mathcal{R}a$ (see Fig. 3). For $\mathcal{R}a$ from 10^7 to 10^9, the DNS profiles for $\mathcal{P}r = 4.38$ are in perfect agreement with the predicted profile (31) for $\mathcal{P}r \gtrsim 1$, while the DNS profiles for $\mathcal{P}r = 2547.9$ are in perfect agreement with the predicted profile (32). On the other hand, the PBP predictions for $\mathcal{P}r = 2547.9$ and $\mathcal{P}r = 4.38$ almost coincide with the PBP prediction for $\mathcal{P}r \gg 1$ and lie well above the corresponding DNS profiles.

In summary, we have derived a new thermal BL equation for turbulent RBC for $\mathcal{P}r > 1$ using the idea of an eddy thermal diffusivity, which close to the plate is shown to depend on the cubic power of the distance from the plate. We have solved the equation to obtain two analytical mean temperature profiles for $\mathcal{P}r \gtrsim 1$ and $\mathcal{P}r \gg 1$ respectively, and demonstrated that they are in excellent agreement with the DNS profiles. The general dependence of the coefficient a and thus the temperature profile (24) on $\mathcal{P}r$, $\mathcal{R}a$, and the geometrical characteristics of the convection cell will be explored in future studies.

The authors OS, SH, and SW acknowledge financial support of the Deutsche Forschungsgemeinschaft (DFG) under the grants SH405/3 and SFB 963/1, project A6, and the Heisenberg fellowship SH405/4 while the work of ESCC is supported by the Hong Kong Research Grants Council under Grant No. CUHK-400311. The authors thank also the Leibniz–Rechenzentrum (LRZ) in Garching for providing computational resources on SuperMUC.

* Olga.Shishkina@ds.mpg.de
† present affiliation: Department of Mathematics, Imperial College London, London SW7 2AZ, UK
‡ Ching@phy.cuhk.edu.hk

[1] B. Castaing, G. Gunaratne, F. Heslot, L. Kadanoff, A. Libchaber, S. Thomae, X.-Z. Wu, S. Zaleski, and G. Zanetti, J. Fluid Mech. **204**, 1 (1989).
[2] E. Siggia, Annu. Rev. Fluid Mech. **26**, 137 (1994).
[3] G. Ahlers, S. Grossmann, and D. Lohse, Rev. Mod. Phys. **81**, 503 (2009).
[4] D. Lohse and K.-Q. Xia, Annu. Rev. Fluid Mech. **42**, 335 (2010).
[5] F. Chillà and J. Schumacher, Eur. Phys. J. E **35**, 58 (2012).
[6] S. Grossmann and D. Lohse, J. Fluid Mech. **407**, 27 (2000).
[7] R. J. A. M. Stevens, E. P. van der Poel, S. Grossmann, and D. Lohse, J. Fluid Mech. **730**, 295 (2013).
[8] L. Prandtl, in *Verhandlungen des III. Int. Math. Kongr., Heidelberg, 1904* (Teubner, Leipzig, 1905) pp. 484–491.
[9] E. Pohlhausen, Z. Angew. Math. Mech. **1**, 115 (1921).
[10] L. D. Landau and E. M. Lifshitz, *Fluid Mechanics*, 2nd ed., Course of theoretical physics, Vol. 6 (1987).
[11] O. Shishkina and A. Thess, J. Fluid Mech. **663**, 449 (2009).
[12] N. Shi, M. S. Emran, and J. Schumacher, J. Fluid Mech. **706**, 5 (2012).
[13] J. D. Scheel, E. Kim, and K. R. White, J. Fluid Mech. **711**, 281 (2012).
[14] R. J. A. M. Stevens, Q. Zhou, S. Grossmann, R. Verzicco, K.-Q. Xia, and D. Lohse, Phys. Rev. E **85**, 027301 (2012).
[15] M. Kaczorowski, O. Shishkina, A. Shishkin, C. Wagner,

and K.-Q. Xia, in *Direct and Large-Eddy Simulation VIII*, edited by H. Kuerten et. al. (Springer, 2011) pp. 383–388.
[16] Q. Zhou and K.-Q. Xia, Phys. Rev. Lett. **104**, 104301 (2010).
[17] V. M. Falkner and S. W. Skan, Phil. Mag. **12**, 865 (1931).
[18] O. Shishkina, S. Horn, and S. Wagner, J. Fluid Mech. **730**, 442 (2013).
[19] O. Shishkina, S. Wagner, and S. Horn, Phys. Rev. E **89**, 033014 (2014).
[20] S. Wagner, O. Shishkina, and C. Wagner, J. Fluid Mech. **697**, 336 (2012).
[21] J. Bailon-Cuba, O. Shishkina, C. Wagner, and J. Schumacher, Phys. Fluids **24**, 107101 (2012).
[22] O. Shishkina and C. Wagner, J. Turbulence **13**, 1 (2012).
[23] B. I. Shraiman and E. D. Siggia, Phys. Rev. A **42**, 3650 (1990).
[24] E. S. C. Ching, Phys. Rev. E **55**, 1189 (1997).
[25] S. Grossmann and D. Lohse, Phys. Fluids **24**, 125103 (2012).
[26] G. Ahlers, E. Bodenschatz, and X. He, J. Fluid Mech. **758**, 436 (2014).
[27] O. Shishkina, C. Wagner, C. R. Mecanique **333**, 17 (2005); O. Shishkina, C. Wagner, Comp. Fluids **36**, 484 (2007); S. Horn et. al., J. Fluid Mech. **724**, 175 (2013), .
[28] U. Schumann, J. Comput. Phys. **18**, 376 (1975); L. Schmitt, R. Friedrich, Notes Num. Fluid Mech. **20**, 355 (1988); C. Wagner et. al., Phys. Fluids **6**, 1425 (1994), .
[29] O. Shishkina, R. J. A. M. Stevens, S. Grossmann, and D. Lohse, New J. Phys. **12**, 075022 (2010).